

# Characterisation of an Energy Absorbing Foam for Motorcycle Rider Protection in LS-DYNA

Steffen Maier<sup>1</sup>, Martin Helbig<sup>2</sup>, Holger Hertneck<sup>3</sup>, Jörg Fehr<sup>1</sup>

<sup>1</sup>Institute of Engineering and Computational Mechanics (ITM), University of Stuttgart

<sup>2</sup>DYNAmore GmbH

<sup>2</sup>SAS-TEC GmbH

## 1 Introduction

A study on traffic fatalities [1] shows that the most frequent causes of motorcyclists' deaths in accidents are multiple skeletal and visceral injuries. Brain and skull injuries are the second leading cause. An injury frequency and pattern data analysis of discharged riders of powered two-wheelers from hospitals [2] show that the most common injuries of non-fatal accidents are injuries of the lower extremities followed by upper extremity and traumatic brain injuries. With this data of fatal and non-fatal accidents it can be said that besides head protection, the protection of a two-wheeler rider's whole body with lower and upper extremities is of major importance.

Current passive safety systems of motorcyclists are dominated by personal protective equipment. This includes helmets, safety clothing and protectors, and more recently, wearable airbag devices. Protectors worn on the limb joints, as well as on the back and tailbone, are protective elements adapted to the shape of the body, which are made of shock-absorbing materials and aim to mitigate hard impacts. These can be worn individually or are often integrated into protective suits. Their protective effect, the reduction of peak loads submitted onto the human body, can be divided in

- internal dissipation of impact energy within the protector,
- delayed transfer of impact energy over a longer period of time,
- and distributed transfer of impact energy over a larger area.

Among other materials used for body protectors, such as hard plastics and silicones, energy absorbing foams are used. Their advantage is that they are light and soft and therefore very comfortable to wear while on fast impacts they're intended to respond very firm to provide good protection.

As part of an effort to investigate a novel safety concept for motorcycles we want to explore another application for such energy absorbing foams to protect motorcycle riders. The novel safety concept restrains the rider to the motorcycle with thigh belts and a newly designed motorcycle body, equipped with multiple airbags and impact protectors to cushion the rider from impacting the motorcycle. The goal of the novel concept is to guide and control a rider's trajectory and energy similar to occupant restraint systems for passenger cars. The objective of the work presented here is to numerically characterise a foam currently used in protective clothing for motorcyclists in LS-DYNA for the proposed impact protectors attached to a motorcycle cockpit. LS-DYNA provides material models that support near test conditioning but still require surface fit or interpolation of test data from dynamic test setups. The novelty of the demonstrated procedure is a polynomial representation of experimental test data that incorporates material card requirements and material behaviour knowledge implemented through constraints in a quadratic objective function. The characterised materials are then used in accident simulations of the proposed safety concept in representative scenarios of real-world accidents.

## 2 Material Card Characterisation

The selected energy absorbing foam material is advertised as a viscoelastic material with very good impact absorption properties with various densities between 200 and 425 g/l. The polyurethane foam has a mixed open and closed cell structure, which gives it its rate-dependent mechanical properties. When a load is applied, the air of the open foam bubbles is forced out through small openings. When the load is removed, the air flows back in. This leads to an adaptive damping behaviour. Under rapid impact, the foams react with high resistance aimed for good protection, while it yields gently under slow impact, i.e., similar to a non-Newtonian fluid. Applied in a wide range of protector products for two-wheelers and horse riders, these can achieve the highest rating of the norms EN 1621-1:2012 for motorcycle limb joint [3] and EN 1621-2:2014 for back protectors [4]. By using vegetable oils for the polyol portion, the percentage of renewable resources in the foam is about 60%.

LS-DYNA provides a variety of material models to capture the behaviour of foams, such as rate dependent loading and hysteretic unloading. In addition to the best possible quality and accuracy in the representation of the material behaviour the model should be well suited to be mapped with near test data and to be calibrated in a simple and understandable way. **MAT\_FU\_CHANG\_FOAM** is suitable for low and medium density foams, has shown to be a reasonable choice to be a starting point for an initial characterisation, is frequently used for a wide variety of foam materials [5, 6] and is therefore chosen.

The goal is to characterise the energy absorbing foam material with a density of 425 g/l. As outlined in [7], but only very briefly summarised, the loading behaviour of the material is derived by surface and curve fitting measurement data with a pendulum impactor test setup. The unloading behaviour is approximated by a parameterised damage formulation. Finally, the quality of the models is tested in a drop tower test setup, which is used to certify body-worn protectors for motorcyclists, e.g., according to EN 1621.

## 2.1 Loading Behaviour

The chosen material model **MAT\_FU\_CHANG\_FOAM** requires engineering stress vs. engineering strain data as a function of multiple constant strain rates. Dynamic tests are conducted with a pendulum impactor dropped from an initial height  $h_0$ , as shown in Fig. 1, with force measurement via the impactor's mass and its acceleration and the displacement via the rotary angle  $\psi$  of the impactor arm. Quasi-static tests are conducted with a universal testing machine. Conditioned foam specimens (23°C and 50% relative humidity for more than 24 hours) with width and length of 20 mm and thickness of 10 mm are measured five times for three dynamic strain rates with impact velocities of  $v_1 = 0.5, 1.5$  and  $4.5$  m/s and one very slow constant loading and unloading velocity of  $v_{const.} = 1$  mm/s. From these measurements stress vs. strain vs. strain rate curves are derived as shown in Fig. 2. As shown, the quasi-static measurements do not form a closed loop but cut off during unloading because the impactor detaches from the foam samples due to the very slow unloading reaction of the foam samples.

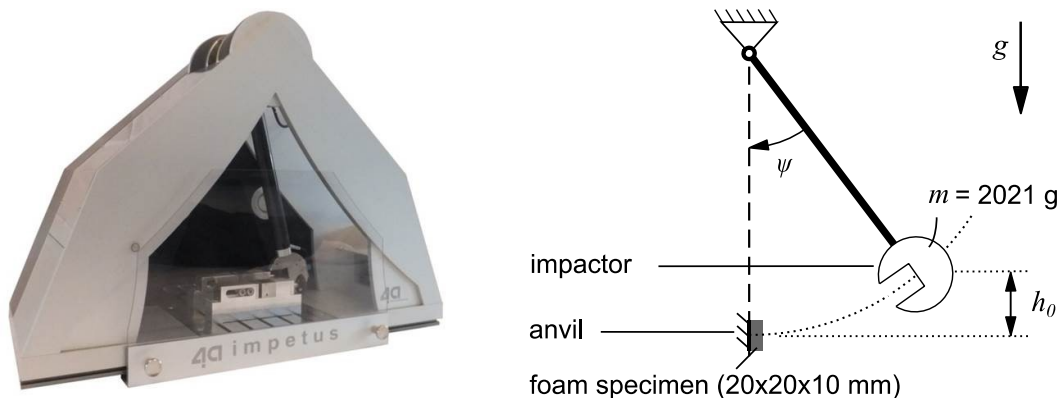


Fig.1: Dynamic pendulum impactor test setup.

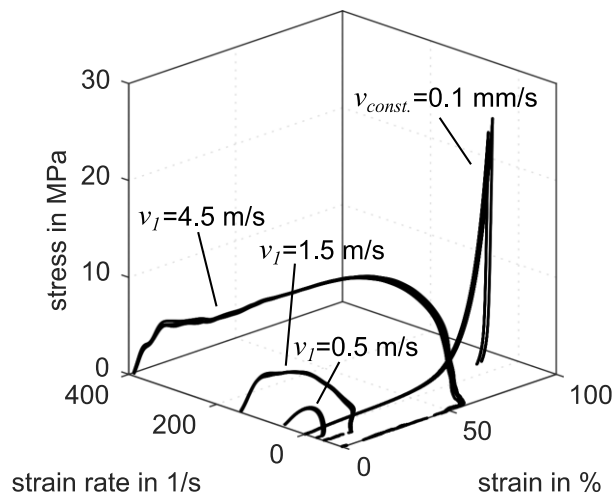


Fig.2: Dynamic and quasi-static test measurement data.

To derive stress vs. strain curves for the required constant strain rates the dynamic and quasi-static measurement data is fitted using bipolynomial and polynomial surface and curve fits. For the 3D surface fit of the dynamic measurement data the stress data points  $z = F(x, y)$  are fitted on non-uniformly spaced rectilinear 2D grid for strain ( $x$ ) and strain rate ( $y$ ) that is logarithmically scaled in strain direction, see Fig. 3. With polynomial coefficients  $\mathbf{b}$  and  $\mathbf{c}$  and with degrees  $n$  in  $x$ -direction and  $m$  in  $y$ -direction this results in

$$z = F(x, y) = (b_0 + b_1x + b_2x^2 + \dots + b_nx^n) \cdot (c_0 + c_1y + c_2y^2 + \dots + c_my^m) \quad (1)$$

Computing, grouping, and renaming the factors for e.g.,  $n = 1$  and  $m = 1$  leads to

$$F(x, y) = a_0 + a_1x + a_2y + a_3xy + a_4y^2 + a_5xy^2, \quad (2)$$

where  $\mathbf{a}$  approximates the  $k$  stress measurement data points  $\mathbf{z}$

$$\underbrace{\begin{bmatrix} z_1 \\ z_2 \\ \vdots \\ z_k \end{bmatrix}}_{\mathbf{z}} \approx \underbrace{\begin{bmatrix} 1 & x_1 & y_1 & x_1y_1 & y_1^2 & x_1y_1^2 \\ 1 & x_2 & y_2 & x_2y_2 & y_2^2 & x_2y_2^2 \\ \vdots & \vdots & \vdots & \vdots & \vdots & \vdots \\ 1 & x_k & y_k & x_ky_k & y_k^2 & x_ky_k^2 \end{bmatrix}}_{\mathbf{A}} \cdot \underbrace{\begin{bmatrix} a_0 \\ a_1 \\ a_2 \\ a_3 \\ a_4 \end{bmatrix}}_{\mathbf{a}}. \quad (3)$$

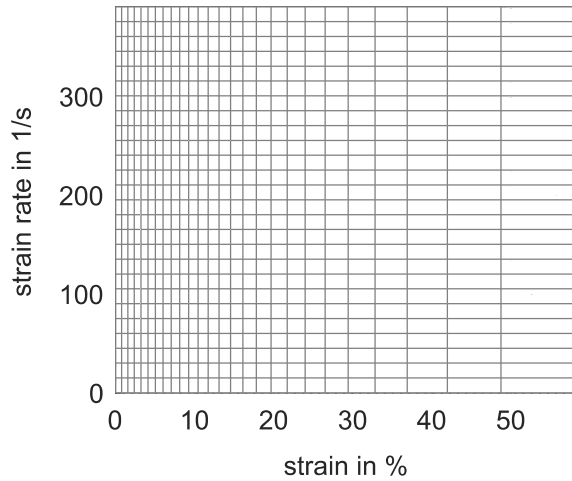


Fig. 3: Tessellation of rectilinear grid with logarithmic scale in strain direction.

The coefficients  $\mathbf{a}$  are determined through the minimisation of a quadratic objective function with linear equality and inequality constraints

$$\min_{\mathbf{a}} \|\mathbf{z} - \mathbf{A}\mathbf{a}\|_2 \text{ s.t. } \begin{cases} F(0, y) = 0 \\ \frac{\partial}{\partial x} F(x) > 0 \\ \frac{\partial}{\partial y} F(y) > 0 \\ \frac{\partial}{\partial y} F(y) \leq p_1 \\ \frac{\partial^2}{\partial x^2} F(x) > 0 \text{ for } x > p_2 \cdot x_{max} \text{ with } p_2 \in [0, 1]. \end{cases} \quad (4)$$

This considers `*MAT_FU_CHANG_FOAM` and `*DEFINE_TABLE` card requirements such that

- the surface intersects the strain rate axis,
- the strain vs. strain rate curves do not intersect each other,
- each of strain vs. strain rate curves is monotonically increasing,

and allows incorporating knowledge about surface topology to get a valid surface fit also in areas with sparse or no data by introducing parameters  $p_1$  and  $p_2$  such that

- the slope  $p_1$  is limited in strain direction,
- a positive curvature is ensured in an upper portion  $p_2$  up to the maximal strain  $x_{max}$  in strain direction.

Additionally, a parameter  $p_3$  describes the logarithmic order of the grid in strain direction, shifting the discretisation to sections where the matched surface's curvature is higher and therefore reduces the required polynomial orders for an adequate fit. The eventual material card curves card are sections of the created surface, seen in Fig. 4. The quasi-static loading data is fitted with the same procedure and  $m = 0$ , also depicted in Fig. 4.

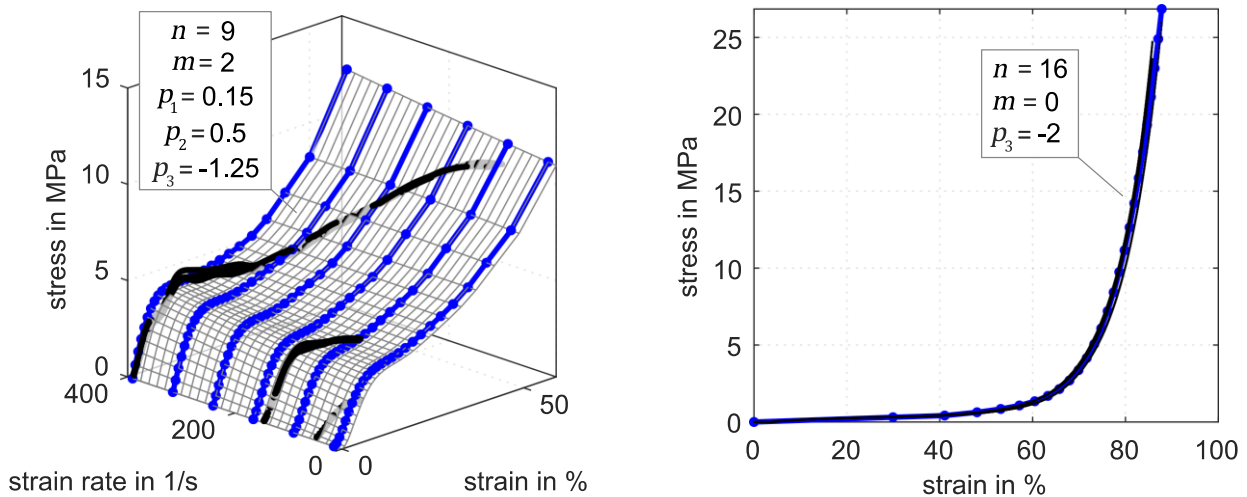


Fig.4: Dynamic loading (left) and quasi-static (right) loading fit of measurement data.

## 2.2 Unloading Behaviour

To model the unloading behaviour, `*MAT_FU_CHANG_FOAM` provides multiple methods. Of these, the method that models rate-dependent unloading, where the unloading response is given by a parameterised damage formulation  $d$  for the principal stresses  $\sigma_i$ , has the most options. The damage formulation based the current and maximal value of the hyperelastic energy  $W$  is

$$\sigma_i = (1 - d)\sigma_i \quad \text{with} \quad d = (1 - \text{HU}) \left[ 1 - \left( \frac{W_{\text{current}}}{W_{\text{maximal}}} \right)^{\text{SHAPE}} \right]^{\text{EXPON}}, \quad (5)$$

where  $\text{HU} \in [0,1]$  is a hysteretic unloading factor, and  $\text{SHAPE}$  and  $\text{EXPON}$  are a shape factor and exponent for unloading [5]. The parameters  $\text{HU}$ ,  $\text{SHAPE}$  and  $\text{EXPON}$  can be tuned by an optimisation, e.g., through `LS-OPT`. In this work they are determined by a parameter variation and equivalent simulation (version `LS-DYNA R9.2.0`) of the dynamic pendulum impactor test setup in such a way that the data fits best for the unloading with the highest load spectrum  $v_1 = 4.5$  m/s, shown in Fig. 5. For loading, the simulation agrees reasonably well except for the zone of initial loading, where the measurements show some oscillation, and for peak stress, where the measurement peaks are less sharp than the simulation stress response. For unloading, the parameters  $\text{HU} = 0.01$ ,  $\text{SHAPE} = 7.5$  and  $\text{EXPON} = 0.5$  allow a good approximation of the measurement with highest load spectrum, while it is not possible to match the unloading paths of all pendulum impact velocities simultaneously.

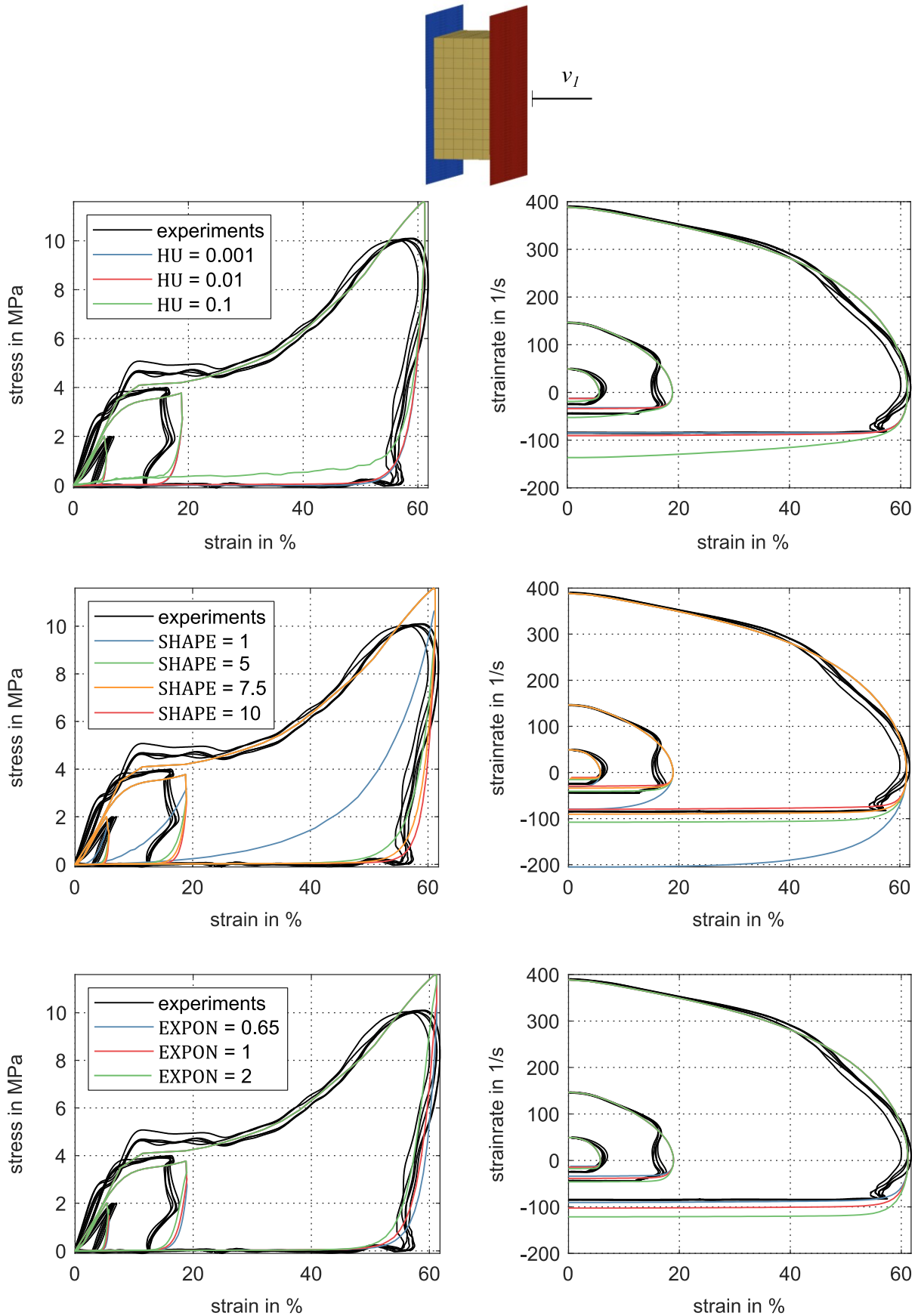


Fig.5: Parameter variation of unloading response with baseline parameters  $HU = 0.01$ ,  $SHAPE = 7.5$  and  $EXPON = 0.65$ .

### 2.3 Drop Tower Tests

The quality of the derived material models is tested with a drop tower test setup. This setup is typically used to quantify and certify the protection performance of motorcyclist limb joint impact protectors worn at shoulders, elbows, forearm, knees, shins and hips according to EN 1621-1:2012 [3] and motorcyclist back protectors according to EN 1621-2:2014 [4] using specified impactors, anvils and drop heights. Here, the setup consists of two different steel drop impactors (Ⓐ:  $m_{\text{Ⓐ}} = 5031$  g, width = 80 mm, depth = 40 mm and Ⓑ:  $m_{\text{Ⓑ}} = 2404$  g, radius = 12.5 mm), dropped from initial heights  $h_0$  with force sensing in the heavy steel anvil and displacement measurement with a motion capture camera system. The foam specimens are 10 mm thick foam sheets and are non-conditioned.

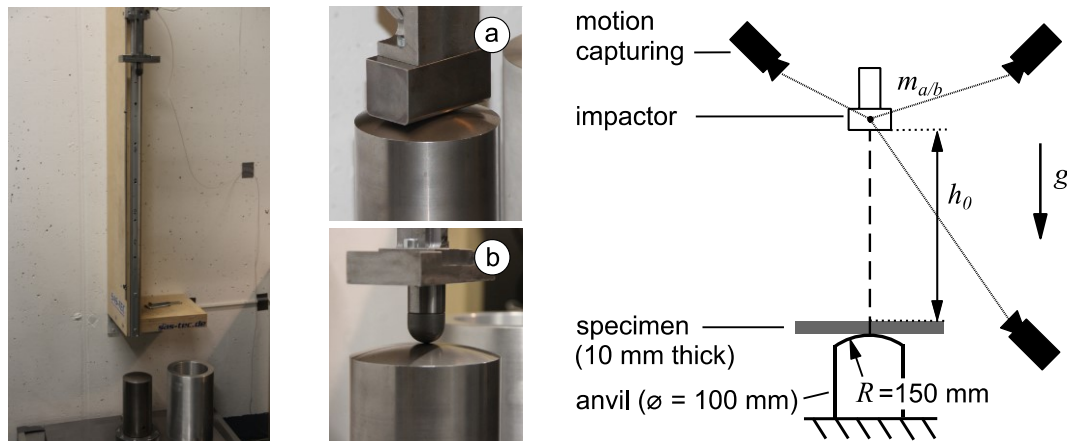


Fig.6: Impactor drop tower test setup.

Tests with impactor Ⓐ and a drop height of 1 m correspond to an impact energy of about 50 J, which is the required impactor geometry, mass and impact energy of EN 1621-1:2012 for limb joint protectors but where a slightly different semicircle anvil geometry with a radius  $R = 50$  mm is specified. If the average transmitted peak force is less than 35 kN, this corresponds to protection level 1; if the average is less than 20 kN, it corresponds to a higher rated protection level 2. Equivalent simulations of the experimental setup are carried out where the impactor hits the foam specimen with an impact velocity that corresponds to the various drop heights in the physical setup. The comparison of the simulation of Ⓐ and three repeated measurements for the foam with density of 425 g/l, depicted in Fig. 7, shows that the force response and the rebound height response for the first impact agrees very well. The subsequent impacts show a significantly higher rebound in the simulation than in the experiment. The achieved maximal strain  $x_{max}$  in this setup is 56 % which is very similar to the maximal strain  $x_{max}$  of 62 % in the dynamic pendulum impactor tests, see Fig. 5.

The comparison of experiments and simulations of impactor Ⓑ for two different drop heights of approximately 0.5 and 1 m show also qualitatively good force response agreement, while the rebound height is higher for the initial impact as well as the subsequent impacts. Here, the reached strains are  $x_{max, \text{Ⓐ}} = 90$  % and  $x_{max, \text{Ⓑ}} = 71$  % and therefore outside the generated material card data which resulted in extrapolation. Video recordings of the experiments as well as the unloading behaviour in the quasi-static test in Fig. 2, show that the material does not immediately adopt the initial geometry after an initial impact and remains temporally compressed. Instead, the viscoelastic foam needs some time to regain its original shape and to release the heat introduced via the impacts. This behaviour is not shown in the simulations. This could explain the different behaviour for the further impacts as the impactor hits the still compressed foam areas in the following impacts. In summary, the comparisons indicate that within the range of the material card curves, the foam force response as well as rebound behaviour can be accurately predicted for the initial impacts.

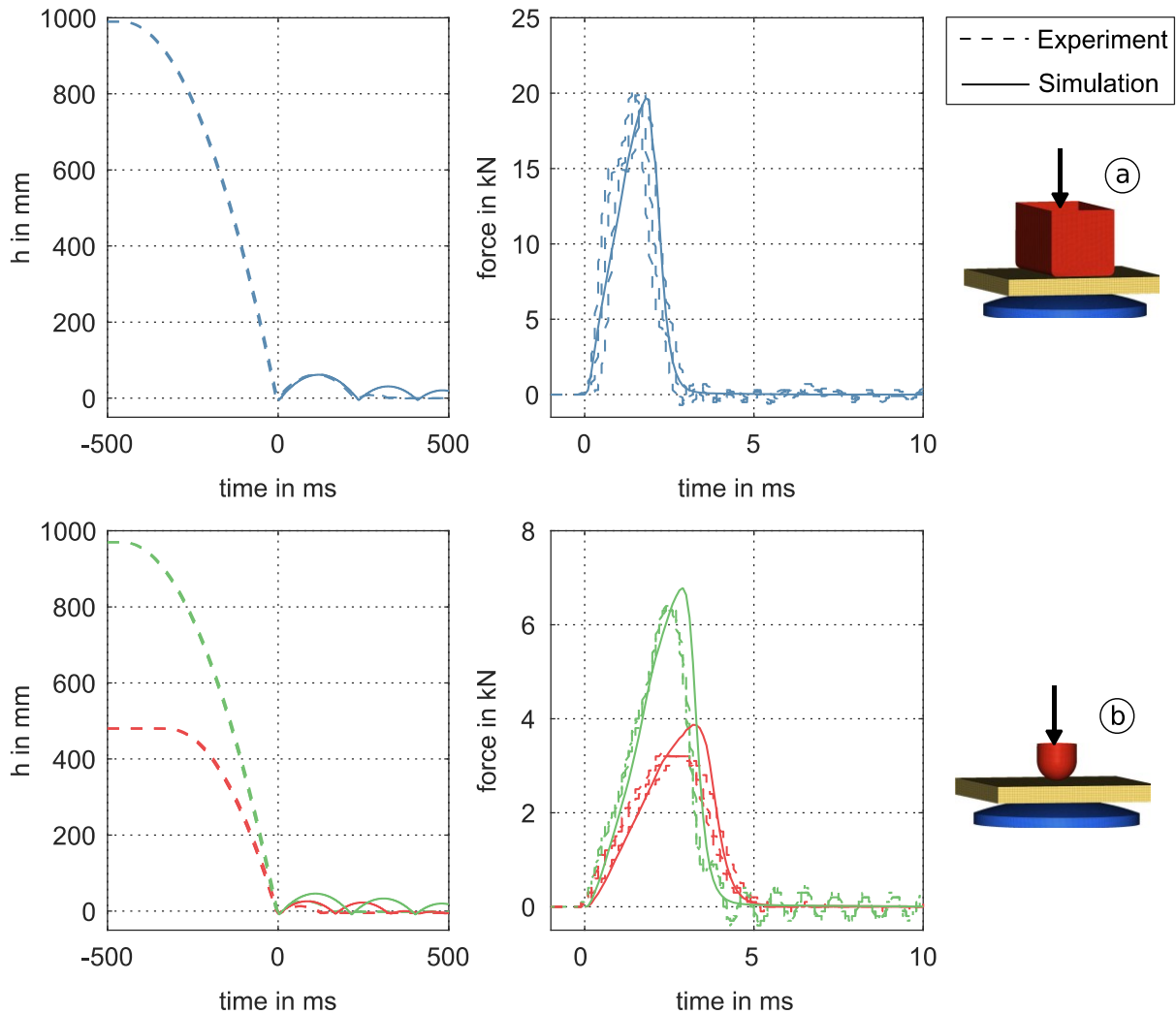


Fig.7: Impactor height and anvil force responses for  $HU=0.01$ ,  $SHAPE=7.5$  and  $EXPON=0.65$ .

### 3 Foam Application for Motorcycle Rider Protection in a Novel Safety Concept

A surrogate model of the novel safety concept and motorcyclist, a 50<sup>th</sup> Hybrid III dummy in sitting configuration is shown in Fig. 8. The concept envisages that in the event of an accident, the rider is restraint to the motorcycle by thigh belts. Surrounding airbags decelerate the rider's body motion and protect the rider from hard contacts with the motorcycle and the accident environment. The foam leg impact protectors reduce the impact forces on the lower extremities. The side impact structure protects the lower extremities laterally. The shown model, introduced in [7], is part of a multi-stage virtual simulation-based development process with models of continuously increasing level of detail and expected fidelity. Trajectories from Madymo multibody simulations [8] are used to represent the accident motion in the finite element simulation, which are implemented as prescribed motions onto a rigid outer body. The prescribed car's body act as reaction surface for the airbags. This methodology corresponds to common simulation strategies of vehicle interior simulations based on crash pulses. The model allows the efficient investigation of sub-questions, such as the evaluation of the performance of the protectors used, with reduced computational costs and model complexity compared to a full finite element model representation.

To evaluate the performance of the leg impact protection with the energy absorbing foam the shown model is simulated in accident scenarios according to norm ISO 13232 [9], which describes representative accident scenarios of motorcycles. The primary contact between dummy and motorcycle is often the knee. Upon frontal impact, axial loading of the femur occurs. On the basis of an evaluation of previous studies on knee, femur and pelvic injuries because of femur axial loading in frontal impacts, [10] recommends values below peak axial forces of 10 kN. To gain some sort of assessment,

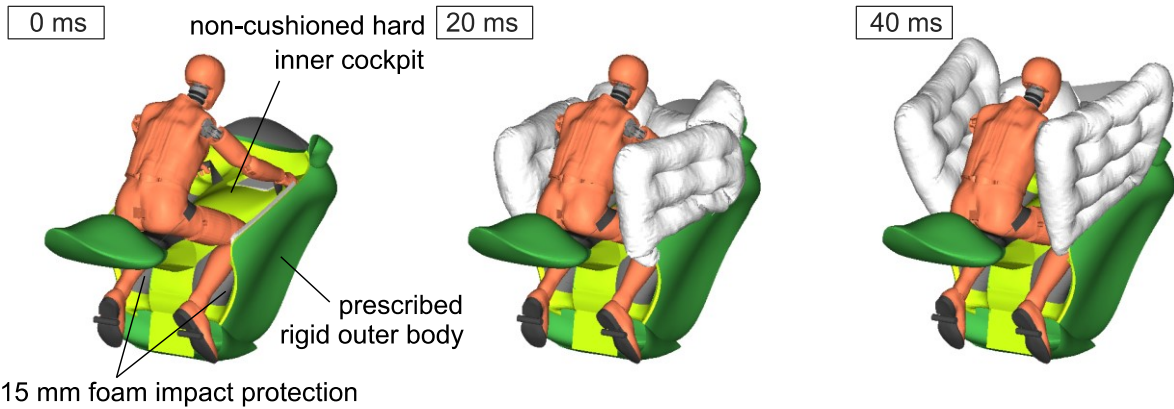


Fig.8: Surrogate model of novel safety concept using imposed multibody motions.

the results for the proposed foam are weight up against simulations without foam which is the non-cushioned inner cockpit surface of 2 mm sheet steel. Simulations of the safety concept showed that femur forces are within the recommended range for all the ISO 13232 scenarios [7]. Fig. 9 and 10 show two of these scenarios where high axial forces occur. Compared to no foam the energy absorbing foam showed an expected improvement in reduced peak loading in both cases. Here, the maximum compression is well within the range of the material card data.

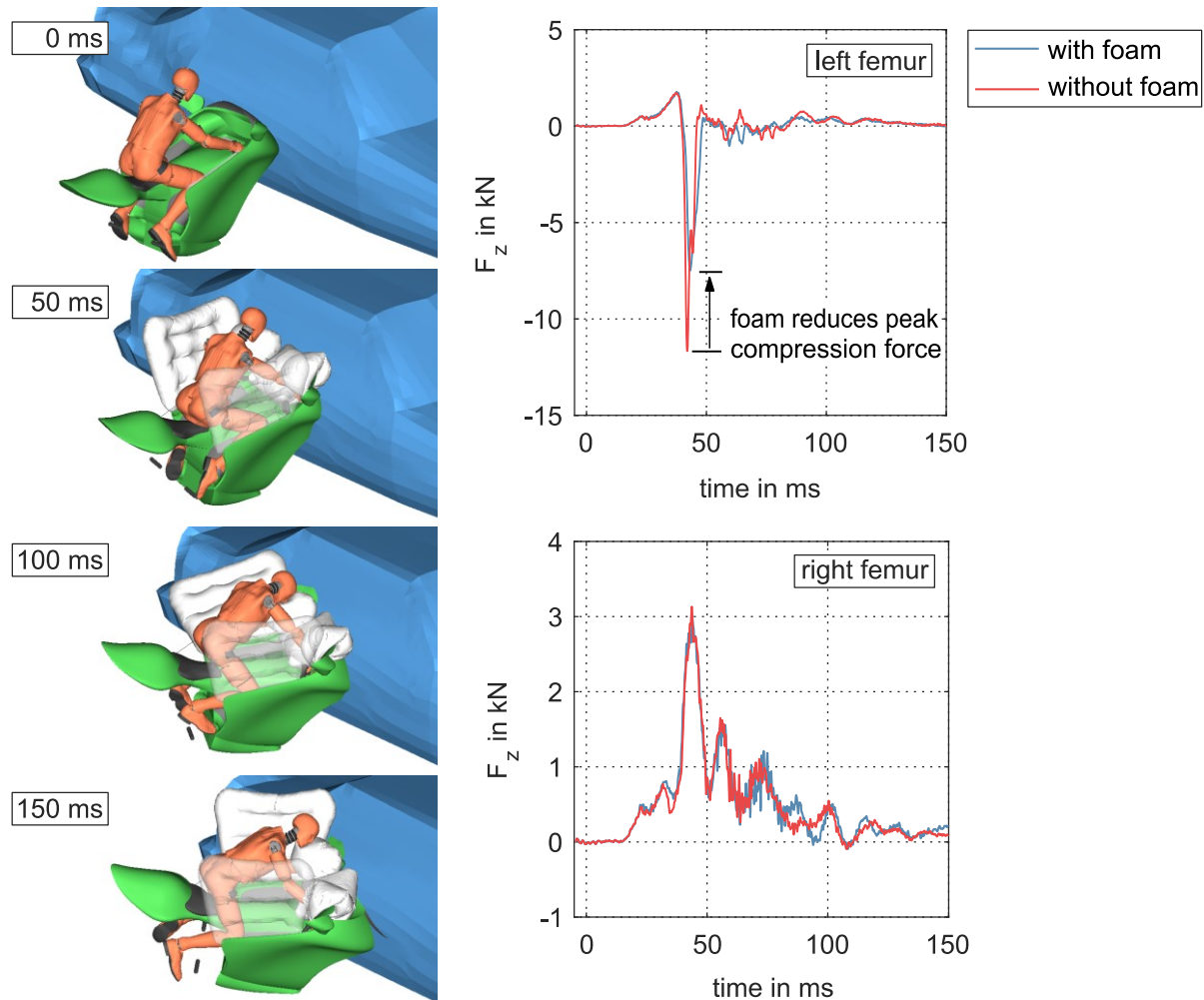


Fig.9: Accident scenario ISO-13232-3 ( $v_{Motorcycle} = 48 \text{ km/h}$ ,  $v_{Car} = 24 \text{ km/h}$ ,  $\theta_{rel} = 90^\circ$ ).



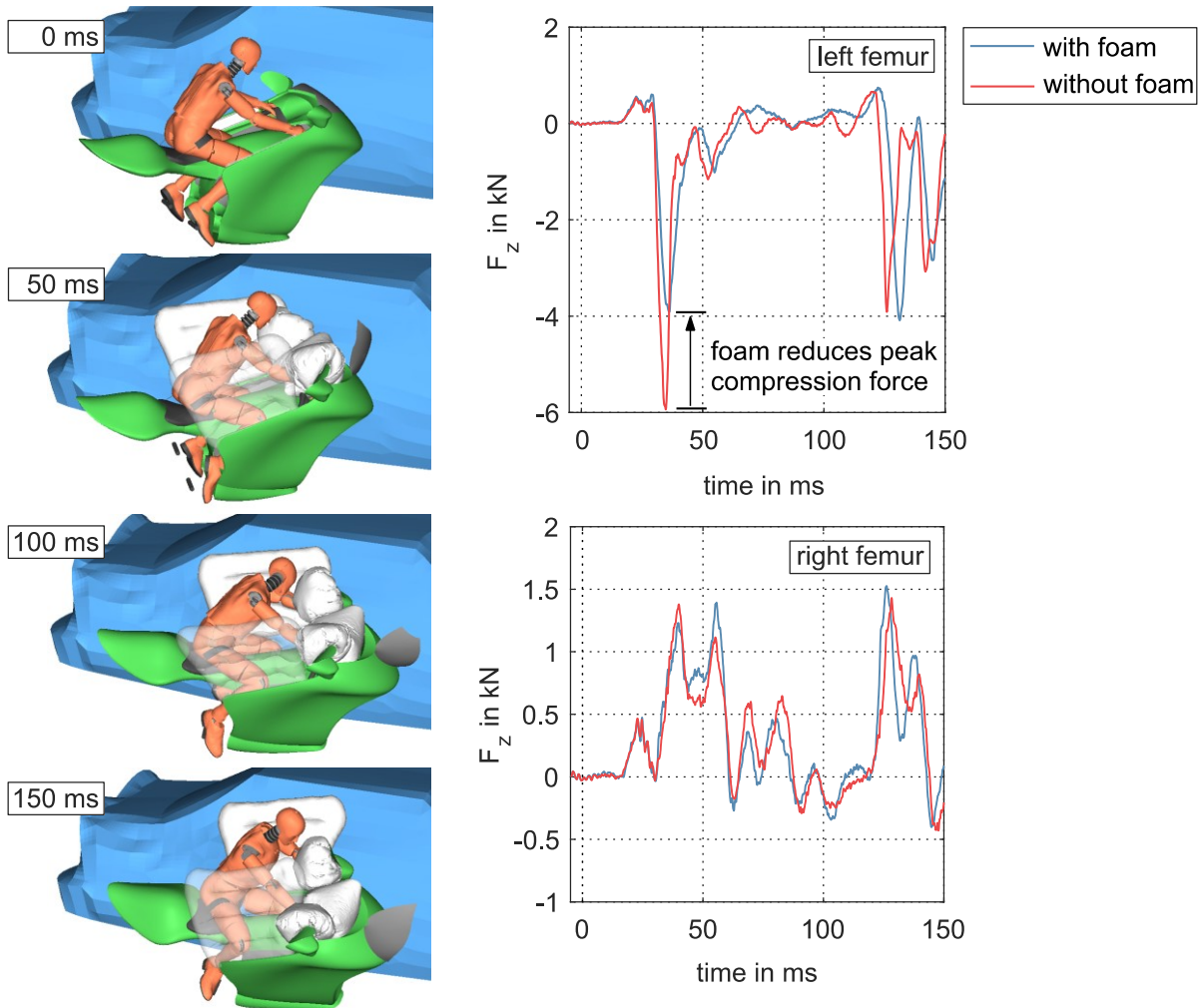


Fig.10: Accident scenario ISO-13232-4 ( $v_{Motorcycle} = 48 \text{ km/h}$ ,  $v_{Car} = 24 \text{ km/h}$ ,  $\theta_{rel} = 45^\circ$ ).

#### 4 Summary

A method to derive stress-strain curves with constant strain rates through polynomial regression of dynamic and quasi-static test data was introduced. Linear equality and inequality constraints ensure that material card requirements are respected, and a valid topology is obtained, while parameters still give the user the possibility to influence the resulting topology to some extent. This can be applied to several material cards. The method was demonstrated for `*MAT_FU_CHANG_FOAM`, which showed promising results in characterising an energy absorbing foam currently used in motorcycle rider personal protection equipment. Thus, using LS-DYNA finite element simulations, it was possible to accurately predict the loading and unloading behaviour of an initial impact within the range of the material card curve data. Outside this area the force response is still estimated well. The novel application of such foam not worn on the body but attached to rider interaction surfaces of a motorcycle performs in the virtual development environment. Compared to a hard reference surface it reduces peak loading associated with knee, femur and pelvic injuries.

#### 5 Acknowledgements

This work is funded by the State Ministry of Baden-Württemberg for Economic Affairs, Labour and Housing Construction within the programme of Innovative Mobility Solutions, and we acknowledge the support by the Stuttgart Center for Simulation Science (SimTech).

## 6 Literature

- [1] Amadesi, A., *et al.*: "The Toll of Traffic-Related Fatalities in a Metropolitan Italian Area through the Experience of the Department of Legal Medicine", *International Journal of Injury Control and Safety Promotion*, Vol. 23, pp. 197–205, 2016.
- [2] Forman, J., *et al.*: "Injuries among Powered Two-Wheeler Users in Eight European Countries: A Descriptive Analysis of Hospital Discharge Data", *Accident Analysis & Prevention*, Vol. 49, pp. 229–236, 2012.
- [3] EN 1621-1:2012: "Motorcyclists' protective clothing against mechanical impact - Part 1: Motorcyclists' limb joint impact protectors - Requirements and test methods", 2012.
- [4] EN 1621-2:2014: "Motorcyclists' protective clothing against mechanical impact - Part 2: Motorcyclists' back protectors - Requirements and test methods", 2014
- [5] LS-DYNA Keywords User's Manual, R9.0, 2016.
- [6] Croop, B., Lobo, H.: "Selecting Material Models for the Simulation of Foams in LS-DYNA", *7<sup>th</sup> European LS-DYNA Conference*, 2009.
- [7] Maier, S., Doléac, L., Hertneck, H., Stahlschmidt, S., Fehr, J.: "Finite Element Simulations of Motorcyclist Interaction with a Novel Passive Safety Concept for Motorcycles", *Proceedings of the IRCOBI Conference*, 2021.
- [8] Maier, S., Doléac, L., Hertneck, H., Stahlschmidt, S., Fehr, J.: "Evaluation of a Novel Passive Safety Concept for Motorcycles with Combined Multi-Body and Finite Element Simulations", *Proceedings of the IRCOBI Conference*, 2020.
- [9] ISO 13232:2005: "Motorcycles – Test and analysis procedures for research evaluation of rider crash protective devices fitted to motorcycles", 2005.
- [10] Berg, F. A., Rücker, P., *et al.*: "Prüfverfahren für die passive Sicherheit motorisierter Zweiräder", *Berichte der Bundesanstalt für Straßenwesen*, 2004.